Heliyon 7 (2021) e06571

Contents lists available at ScienceDirect

Heliyon

journal homepage: www.cell.com/heliyon

Research article

Influence of concentration of anthocyanins on electron transport in dye sensitized solar cells

Alex Okello [a,*], Brian Owino Owuor [b], Jane Namukobe [c], Denis Okello [a], Julius Mwabora [b]

[a] Department of Physics, Makerere University, P.O. Box 7062, Kampala, Uganda
[b] Department of Physics, University of Nairobi, P.O. Box 30197-00100, Nairobi, Kenya
[c] Department of Chemistry, Makerere University, P.O. Box 7062, Kampala, Uganda

ARTICLE INFO

Keywords:
Dye sensitized solar cells
TiO_2
Impedance electron spectroscopy
Slot coating
Fermi level
Recombination resistance
Electron lifetime

ABSTRACT

The influence of concentration of anthocyanins in dye sensitized solar cells (DSSC) has been investigated, with focus on how concentration influence electron transport. The influence on electron transport was then linked to solar cell performance. Anthocyanins were extracted from fresh flowers of *Acanthus pubscenes* using methanol acidified with 0.5% trifluoracetic acid, concentrated using a rotary evaporator and partitioned against ethyl acetate. Concentration of the anthocyanins was determined using Keracyanin Chloride as a standard. DSSC were fabricated using Titanium dioxide as anode, anthocyanins as sensitizers and Platinum as counter electrode material. Titanium dioxide was deposited on Fluorine doped Tin oxide glass substrate using slot coating method. Platinum was deposited on FTO glass substrate using a brush previously dipped in plastisol precursor, and annealed at 450^0C for 20 min to activate Platinum. Dye sensitized solar cells were assembled using anthocyanins at varying concentrations. Performance parameters of the solar cells were measured using a solar simulator which was fitted with digital source meter. Electron transport parameters were studied using electrochemical impedance spectroscopy (EIS). Open circuit voltage, short circuit current and fill factor were observed to increase with concentration of anthocyanins. The increase in solar cell performance was attributed to increase in charge density which led more charges being available for transported to solar cell contacts. The increased charge resulted in a negative shift in Fermi level of electrons in the conduction band of TiO_2. The shift in Fermi level resulted into an increase in open circuit voltage and the overall solar cell performance. EIS studies revealed increase in recombination resistance with concentration of anthocyanins. The increase in recombination resistance was found to be related to increase in electron density, and hence the shift in the Fermi level of electrons in the conduction band of TiO_2.

1. Introduction

The world today is facing a daunting task of mitigating the impact of greenhouse gasses emitted mostly from fossil sources of energy [1]. The greenhouse gasses emitted by the sources have led to global warming, and this has adverse effects on eco systems [2]. Because of the greenhouse gasses, there are now climate changes, and this coupled with growing energy demand and depletion of fossil resources, presents need for sustainable and environmentally friendly energy technology [3]. Fortunately, energy from the sun to the earths is about 3×10^{24}J per year [3]. This amount of energy, when harvested with a suitable technology and converted into electricity can meet all man's energy needs, while at the same time keeping the environment clean [1, 3, 4]. In the last few decades, researchers have therefore embarked on research to design technologies that can be used to harvest this energy [5]. A type of solar cell that has drawn attention since 1991 is the dye sensitized solar cells. It has a low cost of fabrication, and is environmentally friendly, among its' advantages [6].

The basic structure of the dye sensitized solar cell (DSSC) consists of a photoanode and a cathode in between which is a redox electrolyte [6, 7]. The cathode is made of Platinum, while the anode is made of mesoporous Titanium dioxide. Both Platinum and Titanium dioxide are separately deposited on Fluorine doped Tin Oxide (FTO) glass substrate. Titanium is given a sense of light by loading it with a dye [8]. When illuminated, electrons in the dye immediately move from the highest occupied molecular orbital (HOMO) to the lowest unoccupied molecular orbital

* Corresponding author.
E-mail address: alex.okello@mak.ac.ug (A. Okello).

https://doi.org/10.1016/j.heliyon.2021.e06571
Received 13 November 2020; Received in revised form 6 December 2020; Accepted 17 March 2021

(LUMO), and subsequently releases electrons into the conduction band of Titanium dioxide [8, 9]. A redox electrolyte restores the dye back to its original state by donating an electron to the dye. The redox electrolyte is itself restored to its original state, once it receives the electron that was injected in the condition band of Titanium. The use of Platinum at the cathode is to catalyze the transfer of electrons from the external circuit to the redox couple. However, the main disadvantage of the dye sensitized solar cell is their low efficiency. A lot of efforts have been made towards improvement of their efficiency [10]. Some of the areas that have been looked at include; increasing the absorption of light by the solar cells within the electromagnetic spectrum, increasing the distance covered by light through multiple reflection in the photoanode, and many more [11]. As a result, there has been significant increase in efficiency of DSSC, achieving 14.1 % by 2017 [12] for DSSC based on ruthenium-based complexes. However, the ruthenium-based dye solar cells are expensive and secondly, ruthenium metals used in making the dyes are scarce [13]. One the other hand, dyes from natural plants are relatively cheap and are in abundancy. Because of the comparative advantages of natural dyes over the ruthenium-based dyes, there has been numerous researches involving naturals dyes, the world over.

Natural dyes contain light absorbing pigments. The dyes can be extracted from plant leaves, fruits, flowers and stems. The compounds responsible for light absorption in the pigments are anthocyanins, chlorophyll, betalines and many more. These have been variously explored for application in dye sensitized solar cells [1, 11, 14, 15, 16].

Radin studied dye solar cells fabricated using dye extracts from fresh fruits which included; blueberry, blackrasberry, cherry,cranberry, raspberry, strawberry, red grape [17]. The choice of the fruits was based on their total anthocyanins contents. The dyes were extracted using water as solvent. The highest efficiency obtained was 0.17%. Compared to other dyes in the study, this high performance of the dye was attributed to the short distance between the anthocyanin, cyanidin skeleton and the point of attachment to the TiO_2 surface. The short distance facilitates more efficient charge transfer to the anode. In another study, Wuletaw and Delele studied dye solar cells using dye extracts from flowers of *Acanthus sennii chiovenda* and *Euphorbia cotinifolia* [14]. The solar conversion efficiency of the solar cells obtained were 0.15% and 0.136% respectively. The 0.15% efficiency was for a solar cell sensitized using ethanol acidified with 1% HCl. Torchani and colleagues, investigated the performance of dye solar cells using dye extracts from Henna and Mallow. Dye solar cells sensitized using extracts from Mallow had a solar conversion efficiency of 0.215%. Henna based solar cell had a solar conversion efficiency of 0.157% [18]. In addition, Abebe and colleagues used dye extracts from *Teclea shimperi* fruits as sensitizers. The dyes were extracted using different solvents which included water, acidified methanol, acidified ethanol, and acidified water-ethanol mixture at room temperature. The solar cell structure consisted of PEDOT coated FTO counter, TiO_2 based anode, and a qusi-solide state electrolyte. Solar cells sensitized using dyes extracted using acidified ethanol produced the best efficiency of 0.340±0.012%. Raja and co-workers explored the use of dye extracts from *Opuntia dillenii* and *Tamarindus indica* [4]. The dyes were extracted using methanol acidified with 1% HCl. Betalain was extracted from *Opuntia dilleniid* and anthocyanins were extracted from *Tamarindus indica.* The betalain based solar cell had efficiency of 0.47%. Anthocyanins sensitized solar, had an efficiency of 0.14%. The mixture of anthocyanins and betalain in ratio 1:1 by volume produced the best efficiency of 0.2%.

While it is clear that the solar conversion efficiency of solar cells based on natural dyes are very low, we do hypothesize that, the differences in performance are due to variations in concentration of light absorbing compounds in the dyes. The differences in concentration do influence electron transport in different ways, and the result is the differences in solar conversion efficiency.

Dye sensitized solar cells were fabricated based on anthocyanins as sensitizer at varying concentrations. Electron transport was studied using EIS. Electron transport parameters were then used to explain solar cell performances. It was observed that, solar cell performance improves with increase in concentration of anthocyanins. The highest efficiency obtained was 0.145% with concentration of 1.18 mg/ml. EIS studies revealed that, the improvement in solar cell performance was due to increase in recombination resistance at the anode as concentration of anthocyanins increases.

2. Experimental part

2.1. Materials

Methanol, ethyl acetate, acetone,2-propanol, trifluoracetic acid, were purchased locally and were of HPLC grade. Liquid electrolyte (Iodolyte AN-50), platinum catalyst paste (plastisol T/SP), Fluorine doped (FTO) oxide glass substrate ($7\Omega^2$), hot melt sealing film meltonix (60μm) were purchased from Solaronix SA. Kerocyanin chloride, liquid detergent, Helmanex III, TiO_2 nano powder (Degussa P25) comprising of approximately 30% rutile, and 70% anatase, Triton X-100, glass wool and polyethylene glycol (M.W 10,000) were purchased from Merck.

2.2. Materials preparation and anthocyanins extraction

Fresh flowers of *Acanthus pubscens* were collected from Matugga along Bombo road side, in Wakiso district, in central Uganda. Confirmation of the plant type was done at Makerere University Herbarium in the department of Plant Science, Microbiology and Biotechnology. Fresh flowers (200g) of *Acanthus pubscens* were macerated in methanol (700ml) acidified with 0.5% trifluoracetic acid for 24 hours. The soaked flowers were sieved and filtered with a funnel fitted with glass wool to obtain 500 ml of crude extract. The filtrate was concentrated using a rotary evaporator set at 30 °C to obtain 40mls. The reason for concentration was to expel methanol, a polar solvent that cannot be partitioned against ethyl acetate [19]. 40 mls were partitioned against ethyl acetate in a separating funnel. The lower layer contained mainly anthocyanins, while the upper layer contained mainly chlorophylls, flavanols, carotenes and polyphenols [20]. The two layers were separated using a separating funnel, and the upper layer discarded. Excess ethyl acetate in the aqueous layer was expelled by subjecting the sample to rotary evaporation for a short time again, and 27mls was recovered. 27 ml of the concentrated sample was divided and transferred into four amber bottles, each carrying 5mls. The amber bottles helped to protect the anthocyanins from light degradation. To each of the four samples was added 20mls, 35mls, 50mls and 65mls of methanol acidified with 0.5% trifluoracetic acid.

2.3. Preparation of calibration curve

The major anthocyanin in *Acanthus pubscene* is cyanidin rutinoside [21]. To determine the concentration of anthocyanins in the dye samples, Kercyanin Chloride standard was used. 0.114 mg, 0.226 mg, 0.329 mg, 0.467 mg and 0.569 mg of Kercyanin Chloride was measured using an electronic balance. The different masses were each dissolved in 10ml of deionized water. Their absorbance was determined at 530 nm using a Jenway spectrophotometer (Model 7305, UK).

2.4. Preparation of electrodes

FTO glass substrates were dipped in a bath of helmanex III (1%) for 20 min in an ultrasonic bath and later rinsed three times with deionized water. Finally, the electrodes were bathed in ultra-sonic bath of acetone for 20 min and 2-propanol for 20 min.

Titanium paste was prepared by blending 4g of commercial TiO_2 nanopowder, 8ml of 0.1M nitric acid solution and polyethylene glycol and Triton X-100. The mixture was completely ground in porcelain mortar to form a paste [15]. The prepared TiO_2 paste was deposited by slot coating [14]. Deposition was on the conducting side of the FTO glass substrate, on an of area 36 mm^2, defined by a scorch tape. The deposited

TiO_2 was annealed at 450 °C in an open-air tube furnace (Labtech, model LEEF-4025-3) for 20 min. When it had cooled to about 30 °C, the anodes were dipped in anthocyanins at varying concentrations and left to absorb the anthocyanins for 16 hours.

The cathode was prepared by coating FTO glass substrates with a Platinum. An art brush was dipped in plastisol, a platinum precursor and applied onto the FTO glass substrate. Platinum catalyst was activated by annealing in the tube furnace for 20 min. The counter electrodes were left to cool naturally in air.

2.5. Assembly of solar cells

The anodes, loaded with the dyes were picked from their holders and washed with ethanol. The anodes were placed with conducting side facing up. Meltonix, cut with a hole of about 8mm by 8mm was placed such that, the deposited TiO_2 loaded with the dye was within the hole. The prepared counter electrode, was placed on top of the anode such that, contacts to the solar cells were sufficient for applying copper tape to improve electrical contact, and connecting crocodile clips. Sealing was done by use of a hot solder iron, pressed ontop of the counter electrode, along the edges of the solar cell. The electrolyte, Iodolyte-AN 50 was injected into two holes behind the counter electrode, and the holes sealed with cell cups and meltonix as before.

2.6. Measurement of photovoltaic performance and electron transport

Using a solar simulator, intensity of light was set at $1000Wm^{-2}$. A Keithley instrument (Model 2400,4066884, C32) was used to measure open circuit voltage, short circuit current, fill factor.

Electrochemical impedance spectroscopy (EIS) was done using an Autolab PGSTAT 204. A voltage of 0.7V was applied to the solar cells, and frequency was set to vary from 1Hz to 1MHz.

3. Results and discussion

3.1. Calibration curve and absorption properties of anthocyanins

The absorbance values of standard solutions at varying concentrations were measured at 530 nm.Absorbance was plotted against concentration (Figure 1) using matlab software.

As predicted by the Lambert-Bear law, there is a linear relationship between absorbance and concentration [16].

Absorbance of anthocyanins were now measured at 530 nm together with their spectra. The results were plotted using matlab as before, and the spectra is presented in Figure 2.

Using the equation $y = 0.078x + 0.039$, absorbance values were used to compute concentration of the dye samples. These were; a:0.4 mg/ml; b:0.6 mg/ml; c:1.0 mg/ml; and d:1.18 mg/ml.

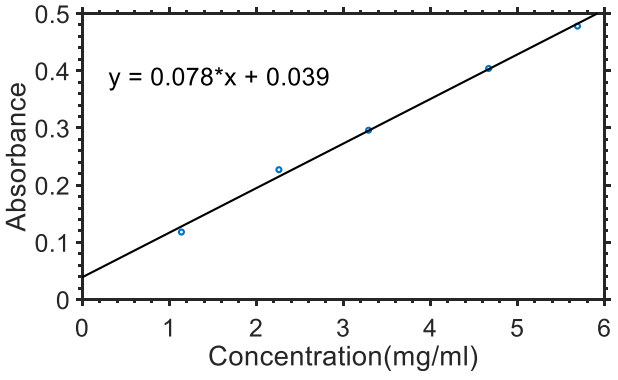

Figure 1. Absorbance-concentration curve for the Kercyanin Chloride standard solutions. The equation inset relates absorbance to concentration. y: Absorbance; x: concentration (mg/ml).

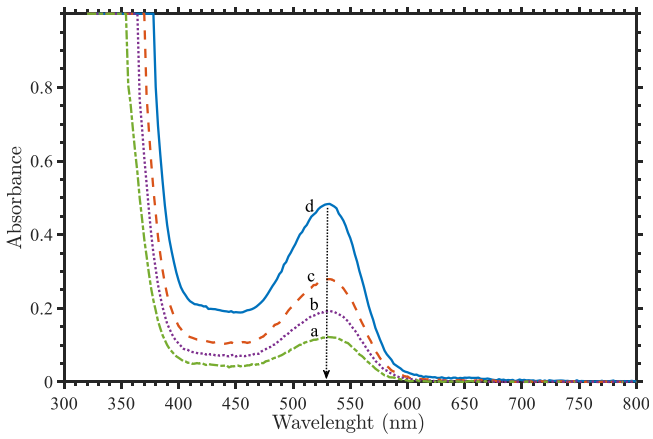

Figure 2. UV-vis spectra for dyes at varying concentrations; a:0.4 mg/ml; b:0.6 mg/ml; c:1.0 mg/ml; and d:1.18 mg/ml. The arrow represents absorbance picks for the different concentrations at 530 nm.

From the UV-vis spectra, Figure 2, all the absorbances peak at approximately 530 nm. This is consistent with results obtained by Namukobe (2006). In an acidic medium, dye extracts with mainly anthocyanins are known to have absorbance peaks at 530 nm [22]. This indicates that, the dye extracts contains mainly anthocyanins. In addition, as concentration increases, the area under the spectra increases. This means the dye is able to absorb more photons as concentration increases. Furthermore, at 530 nm, the peaks increase with concentration. This observation is consistent with the Lambert-Bear law, a linear relationship between absorbance and concentration for a given pathlength of light [16].

3.2. Photovoltaic performance

Performance parameters, namely; open circuit voltage (V_{oc}), short circuit current (I_{sc}), and fill factor (FF), were measured. Conversion efficiency (η) was computed using the relation; $\eta = V_{oc} \times J_{sc} \times FF \times 100/P_{in}$; where, J_{sc} is current density, P_{in} is the power of light incident onto the solar cells [23]. The results are presented in Figure 3 and Table 1.

Table 1 shows that except for the solar cell for which concentration of anthocyanins was lowest; **a:**0.4 mg/ml, open circuit voltage, short circuit density, fill factor and efficiency all increase with increase in concentration of anthocyanins. Maximum efficiency of 0.145% is obtained at maximum concentration, d. The corresponding; open circuit voltage is 0.468V, short circuit current density:5.333 mA/cm^2, and fill factor: 0.582. Increase in fill factor is observed to be marginal, becoming better

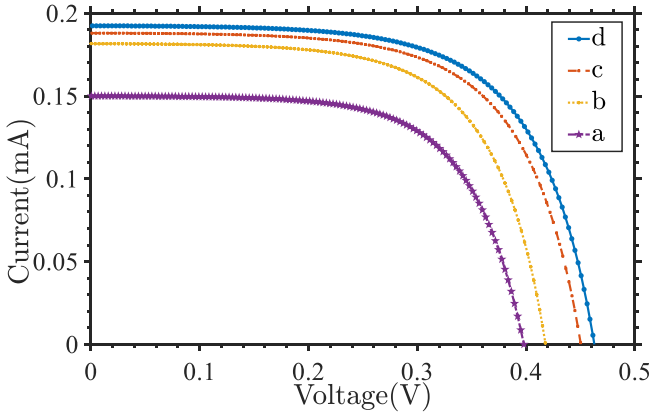

Figure 3. Current-Voltage (I–V) curves for the dye sensitized solar cells showing the influence of anthocyanins on solar cell performance at 1 sun. a:0.4 mg/ml; b:0.6 mg/ml; c:1.0 mg/ml; and d:1.18 mg/ml.

at higher concentration. The marginal increase is probably due to marginal increase in short current density.

Table 2 is a summary of selected studies done on solar cells using natural dyes and an N3 synthetic dye.

Performances in Table 2 shows that, dye sensitized solar cells based on natural dyes are generally low. In the table, the highest efficiency of a dye sensitized solar cell based on a natural dye is 0.301%. For N3 dye, which is a synthetic dye, the conversion efficiency is 4.05%. The poor performance of solar cells based on natural dyes have been attributed to probably poor interaction of natural dyes with TiO_2 surface.

3.3. Discussion of increase in solar cell performance

The increase in short current density as concentration increases can be attributed to increased absorption of light [26]. The increased absorbance of photons leads to increased photogenerated electrons (charge density) resulting into more current.

Open circuit voltage increases because of a shift in Fermi level of electrons in the conduction band of TiO_2 [27]. To explain the shift in Fermi level of electrons in the conduction band, we consider the definition of open circuit voltage given by Eq. (1) [28].

$$V_{oc} = \frac{E_{cb}}{e} + \frac{kT}{e}\ln\left(\frac{n}{N_{cb}}\right) - \frac{E_{red}}{e} \quad (1)$$

where; E_{cb} is the Fermi level of electrons in the conduction band of TiO_2, e is the electron charge, k is the Boltzmann constant, T is temperature of the semiconductor material (TiO_2), N_{cb} is the density of states, n is the number of electrons injected in the conduction band of the conduction band of TiO_2 and E_{red} is the redox potential of the electrolyte. The first two terms on the right-hand side of Eq. (1) is collectively called the quasi Fermi level of electrons in the conduction band of TiO_2. This quasi Fermi level is influenced by the number of electrons, n injected into the conduction band of TiO_2 [28]. Because n is always less than N_{cb} , when n becomes large at high concentration of anthocyanins, the term $(kT/e)\ln(n/N_{cb})$ approaches zero. The open circuit voltage is then approximated by Eq. (2) [29].

$$V_{oc} \approx \frac{E_{cb}}{e} - \frac{E_{red}}{e} \quad (2)$$

There is a difference of the term $(kT/e)\ln(n/N_{cb})$ between Equation 1 and Equation 2. The difference is the shift in Fermi level of electrons in the conduction band of TiO_2 that results into increase in open circuit

Table 1. Performance of the DSSC with varying concentrations of anthocyanins, measured at 1 sun. a:0.4 mg/ml; b:0.6 mg/ml; c:1.0 mg/ml; and d:1.18 mg/ml. V_{oc} (V): open circuit voltage; I_{sc}(mA/cm^2): short circuit current density; FF: fill factor; η (%): solar conversion efficiency.

Concentration (mg/ml)	V_{oc}(V)	I_{sc}(mA/cm^2)	FF	η (%)
d	0.468	5.333	0.582	0.145
c	0.465	5.224	0.577	0.140
b	0.424	5.028	0.524	0.111
a	0.380	5.778	0.620	0.065

Table 2. Summary of performance of selected dyes. V_{oc}(V):open circuit voltage; I_{sc}(mA/cm^2): short circuit current density; FF: fill factor; η (%): efficiency.

Specimen	Major compound present	V_{oc}(V)	I_{sc} (mA/cm^2)	FF	η (%)	Reference
Acanthus pubscens	Anthocyanin (Cyanidin)	0.468	5.333	0.582	0.145	This work
Acanthus senii chio	Not known	0.507	0.491	0.604	0.150	[14]
Blueberry	Anthocyanin (Cyanidin)	0.392	0.96	0.47	0.17	[17]
Canarium odontophyllum	Anthocyanin (Cyanidin)	0.35	9.74	0.546	1.43	[24]
Canarium Odontophyllum	Anthocyanin (Pelargonidin)	0.357	6.57	0.484	0.87	[24]
Opuntia dillenii	Betalain	0.521	1.09	0.69	0.47	[4]
Tamarindus indica	Anthocyanin	0.532	0.35	0.67	0.14	[4]
Red frangipani flowers	Not known	0.495	0.94	0.65	0.301	[25]
-	N3 dye	0.782	8.31	0.62	4.05	[25]

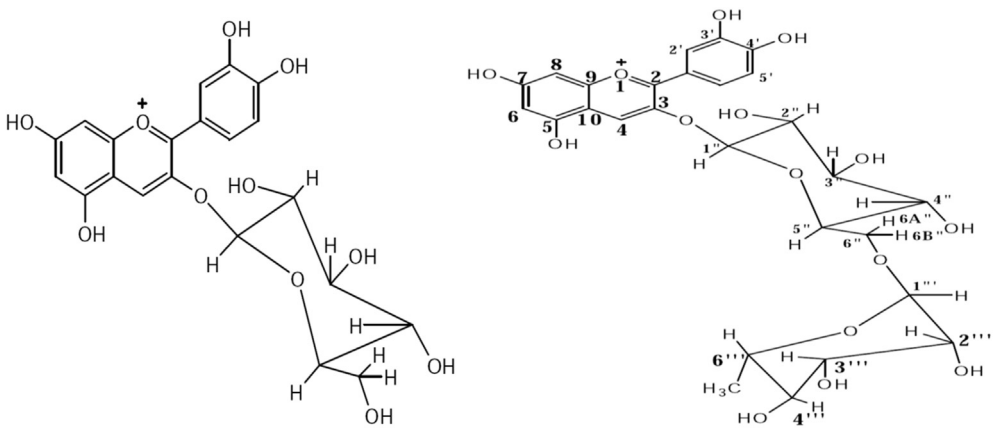

a **b**

Figure 4. a Schematic representation of chemical structure of Cyanidin-3-glucoside and b Scheme of Cyanidin-3-rutinoside [21].

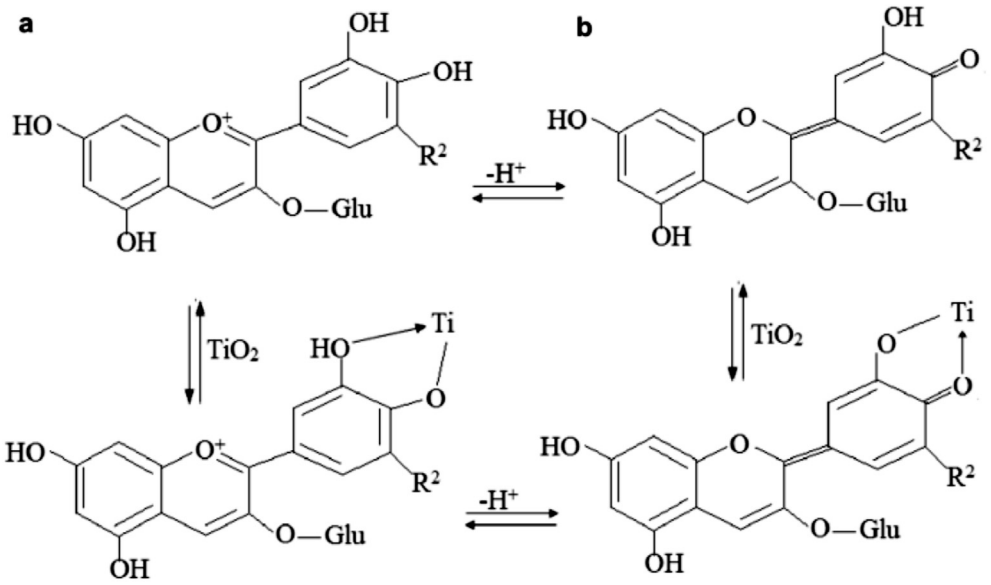

Figure 5. Schematic representation of complexation between cyanidin and TiO_2 surface; a: flavilium form of the anthocyanins; b:quinonoidal form; Glu:glucoside or rutinoside (Adapted from [13] under creative commons licenses [31]).

voltage. Eq. (2) also gives the maximum possible open circuit voltage that can obtained from a dye sensitized solar cell. However, owing to recombination losses, the open circuit voltage obtained is always low [17, 27].

Other factors which affect the quasi Fermi level include; (1) the number of anchoring groups that attached themselves to TiO_2 surface and, (2) type of anchoring group [30]. Anthocyanins extracted from *Acanthus Pubscens* contains two types of anthocyanins, namely; Cyanidin -3-rutinoside (3%) and Cyanidin-3-glucoside (97%) [21]. The structures are shown in Figure 4.

The attachment of cyanidin 3-glucoside onto the semiconductor TiO_2 surface is shown in Figure 5.

The mode of attachment is through bidentate. The adsorption of the dye onto the semiconductor surface acts as a pathway for injecting electrons into the conduction band of TiO_2 [13]. The interaction of these two types of anthocyanins with TiO_2 too probably causes a shift in the Fermi level of electrons in the conduction band [13, 27].

The saturation of short circuit current as well as open circuit voltage as observed from the closeness of I–V curves as concentration increases can be attributed to decrease in electron injection efficiency into the conduction band of TiO_2 as a result of shift in the conduction band, the nature of materials used to construct the solar cells [27] and steric hinderance on the surface of TiO_2 as the concentration of anthocyanins increase [32]. The steric hindrance affects the attachment of dye molecules on the TiO_2 surface and therefore not only affects charge injection in the conduction band of TiO_2 [8,17], but also the Fermi level of electrons in TiO_2.

Both fill factor and solar conversion efficiency are functions of short circuit current and open circuit voltage. Their variations are there for influenced by changes in open circuit voltage and short circuit current.

3.4. Electrochemical impedance spectroscopy

Information about electron transport in the solar cells was investigated using impedance spectroscopy. Figure 6 shows the impedance spectra that was obtained.

Interpretation of the EIS spectra was done in line with the transmission line model [33]. Figure 7 was proposed as the equivalent circuit for the solar cell, and was used to interprete the EIS spectra.

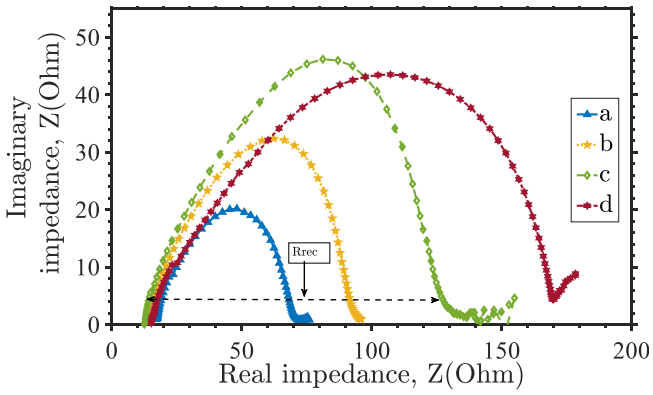

Figure 6. Nyquist plot, a graph of imaginary impedance against real impedance for the solar cells at varying concentrations. a:0.4 mg/ml; b:0.6 mg/ml; c:1.0 mg/ml; and d: 1.18 mg/ml.

Usually, the impedance spectra consist of three arcs [34]. The visibility of the arcs depends on the applied biasing voltage to the solar cell [33]. At some applied voltages, depending on the solar cell, the arcs may overlap one another [35].

In Figure 6, the clearly visible arc is associated with a parallel combination of resistance to recombination, R3 at the anode, and the chemical capacitance C2 of the anode. The diameter of this arc equals R3 [36]. This was measured using EIS spectrum analyzer [37]. The

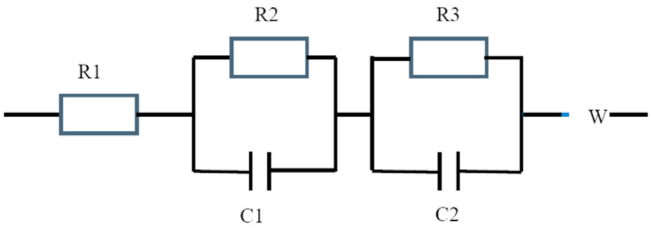

Figure 7. Simplified transmission line model; R1: Series resistance; R2: recombination resistance of counter electrode; R3: recombination resistance of anode; C1: chemical capacitance of anode; C2: Helmholtz capacitance of counter electrode; W: Warburg impendance.

Table 3. Determined electron transport parameters from Nyquist plots. a: 0.4 mg/ml; b: 0.6 mg/ml; c: 1.0 mg/ml; and d: 1.18 mg/ml; R1: series resistance, R3; recombination resistance at anode $R_t(\Omega)$: transport resistance.

Concentration of dye used (mg/ml)	R1(Ω)	R3(Ω)	$R_t(\Omega)$
d	13.02	200.15	213.17
c	12.41	120.19	132.60
b	13.77	81.20	94.97
a	17.51	53.83	71.34

measurement is illustrated on Figure 6 [36, 38]. R1 is read from the first intercept on the real axis. Transport resistance was computed through the relation; $R_t = \mathrm{R1} + \mathrm{R2} + \mathrm{R3}$ [39]. R2 was set to zero because of absence of arcs representing recombination at the counter electrode in Figure 6. The measured and computed parameters are presented in Table 3.

It follows from Table 3, that the solar cell with the lowest concentration has the lowest recombination resistance and lowest transport resistance. The solar cell with the highest recombination resistance and transport resistance is made from the highest concentration of anthocyanins. Thus, recombination resistance and transport resistance is observed to increase with increasing concentration of anthocyanins.

The recombination resistance is defined by Eq. (3) [29].

$$\mathrm{R3} = \left(\frac{\partial j_{rec}}{\partial V_F}\right)^{-1} \approx R_0 \exp\left[\frac{-\beta e V_F}{kT}\right] \tag{3}$$

where; $j_{rec} = j_{sc} - j$ is the current that results from recombination, V_F is the applied voltage corrected for series resistance, β is a coefficient that is related to non-ideality factor, m through $m = 1/\beta$. It defines the loss of charge from TiO_2 to electrolyte. e is the electron charge, k is Boltzmann constant, and R_0 is a parameter which defines activation of recombination. It is defined by Eq. (4)

$$\mathrm{R}_0 = \frac{\sqrt{\pi\lambda kT}}{e^2 L \alpha k_r c_{ox} N_s} \exp\left[\alpha \frac{E_{cb} - E_{red}}{kT} + \frac{\lambda}{4kT}\right] \tag{4}$$

where; L is the thickness of TiO_2, c_{ox} is the concentration of acceptor species in TiO_2, λ reorganization energy of acceptor species, α is a parameter associated with electron traps below the conduction band of TiO_2, k_r is the rate constant for recombination kinetics.

It follows from Eqs. (3) and (4) that, it is R_0 which influences recombination resistance, R3 [40]. We note that, R_0 is its self a function of rate constant for recombination kinetics, k_r , the energy difference, $E_{cb} - E_{red}$, and many other parameters defined in Eq. (4). In a solar cell, all the other parameters are constant except k_r and $E_{cb} - E_{red}$ which depend mostly on the number of electrons injected in the conduction band of TiO_2 [27]. Thus, the increase in recombination resistance can be attributed to increase in R_0, which is directly linked to the number of electrons injected in the conduction band of TiO_2 [29]. It is possible that, increase in recombination resistance leads to increased electron lifetime, and therefore fewer elections do recombine with electron acceptor species [41].

4. Conclusion

Dye sensitized solar cells were fabricated and sensitized using anthocyanins at different concentrations. The concentration of the anthocyanins used were 1.18 mg/ml, 1.00 mg/ml,0.60 mg/ml and 0.40 mg/ml. The solar cells had conversion efficiencies of 0.145%, 0.140%, 0.111% and 0.065% respectively. It was observed that open circuit current density, open circuit voltage, fill factor and solar conversion increase with increase in concentration of anthocyanins. The increase in concentration allows for absorption of more light, and more electrons are exited and injected into the conduction band of TiO_2. This avails more charge for transportation to the solar cell contacts. The increase in charge density is indicated by increase in short current density. The increase in open circuit voltage was attributed to shift in Fermi level of electrons in the conduction band of TiO_2. The Fermi level begins to shift immediately charge density begins to increase.

The shift in Fermi level also led to increase in recombination resistance. The bigger recombination resistance as concentration increased, probably led to longer electron lifetime since fewer electrons recombined with electron acceptor species. More electrons were therefore collected and transported to cell contacts.

Declarations

Author contribution statement

Alex Okello: Conceived and designed the experiments; Performed the experiments; Analyzed and interpreted the data; Wrote the paper.

Brian Owino Owuor: Conceived and designed the experiments; Performed the experiments.

Jane Namukobe: Conceived and designed the experiments; Analyzed and interpreted the data.

Denis Okello: Analyzed and interpreted the data.

Julius Mwabora: Analyzed and interpreted the data.

Funding statement

This work was supported by African Center of Excellency in Materials, Product Development and Nanotechnology (MAPRONANO-ACE), Uganda (003) at Makerere University and International Science Program (ISP) of Sweden, UG 001 project under Materials Science and Solar Energy Network for Eastern and Southern Africa (MSSEESA)

Data availability statement

Data will be made available on request.

Declaration of interests statement

The authors declare no conflict of interest.

Additional information

No additional information is available for this paper.

Acknowledgements

We are grateful to the Department of Physics, University of Nairobi, Kenya for allowing access to their equipment to do this work. We also owe a debt of thanks to Tom Otiti, formerly a Professor of Physics at the Department of Physics, Makerere University for reading through the draft manuscript and providing useful inputs.

References

[1] W.R. Abebe, A.W. Delele, H.G. Nigus, T.A. Yeshitila, Anthocyanin components for dye-sensitized solar cells extracted from Teclea Shimperi fruit as light-harvesting materials, Mat. Sci. Energy Technol. 3 (2020) 889–895.

[2] W.R. Abebe, A.W. Delele, H.G. Nigus, T.A. Yeshitila, Anthocyanin components for dye sensitized solar cells extracted from Teclea shimperi fruit as light harvesting materials, Mat. Sci. Energy Technol. 3 (2020) 889–895.

[3] B. Li, W. Liduo, K. Bonan, W. Peng, Q. Yong, Review of recent progress in solid-state dye-sensitized solar cells, Sol. Energy Mater. Sol. Cell. 90 (5) (2006) 549–573.

[4] R. Ramamoorthy, N. Radha, G. Maheswari, S. Anandan, S. Manoharan, W.V. Rayar, Betalain and anthocyanin dye-sensitized solar cells, J. Appl. Electrochem. 46 (2016) 929–941.

[5] M.M. Ardakani, R. Arazi, Improving the effective photovoltaic performance in dye sensitized solar cells using an azobenzenecarboxylic acid based system, Heliyon 5 (2019), e01444.

[6] B. O'Regan, M. Gratzel, A low cost high efficiency solar cell based on dye sensitization colloidial titanium dioxide films, Nature 353 (1991) 737–740.
[7] M.K. Nazeeruddin, E. Baranoff, M. Gratzel, Dye sensitized solar cells: a brief overview, Sol. Energy (2011) 1172–1178.
[8] Q. Wang, I. Seigo, M. Gratzel, F.F. Santiago, I.M. Sero, J. Bisquert, B. Takeru, I. Hachiro, Characteristics of high efficiency dye sensitized solar cells, J. Phys. Chem. B 110 (2006) 25210–25221.
[9] J. Bisquert, D. Cahen, G. Hodes, S. Ruhle, A. Zaban, Physical chemical principles of photovoltaic conversions with nanoparticulate,mesoporous dye sensitized solar cells, J. Phys. Chem. B 108 (2004) 8106–8118.
[10] M. Berginc, U.O. Krasovec, M. Topic, Solution processed silver nanoparticles in dye sensitized solar cells, J. Mater. Sci. (2014).
[11] N.A. Ludin, A.A. Mahmood, A.B. Mohamad, H.A. Kadhum, K. Sopian, N.S. Karim, Review of natural dye photosensitizers for dye sensitized solar cells, Renew. Energy Sustain. Energy Rev. 31 (2014) 386–396.
[12] N.F.M. Sharif, M.Z.A.A. Kadir, S. Suhaidi, A.R. Suraya, W.W. Hasan, S. Shaban, Charge transport and electron recombination suppression in dye sensitized solar cells using graphene quantum dots, Res. Phys. (2019).
[13] N.Y. Amogne, A.W. Delele, T.A. Yeshitila, Recent advances in anthocyanins dyes extracted from plants for dye sensitized solar cells, Mat. Renew. Sustain. Energy 9 (23) (2020).
[14] A.A. Wuletaw, W.A. Delele, Dye sensitized solar cells using natural dye as light harvesting materials extracted from acanthus senni chiovenda flower and Euphorbia cotinifolia leaf, J. Sci. Adv. Mat. Dev. 1 (2016) 488–494.
[15] S. Hao, J. Wu, Y. Huang, J. Lin, Natural dyes as photosensitizers for dye sensitized solar cells, Sol. Energy 80 (2006) 209–2014.
[16] Z. Arifin, S. Sudjito, D. Widhiyanuriyawan, S. Suyitno, Performance enhancement of dye sensitized solar cells using natural dye sensitizer, Int. J. Photoenergy (2017).
[17] A. Radin, Estimating the impact of dye concentration on photoelectrochemical performance of anthocyanins sensitized solar cells: a power law model, J. Photon. Energy 1 (2011), 011123.
[18] A. Torchani, S. Saadaoui, R. Gharbi, M. Fathallah, Sensitized solar cells based on natural dyes, Curr. Appl. Phys. 15 (2015) 3017–3312.
[19] C. Adaku, I. Skarr, B. Helge, R. Byamukama, M. Jordheim, A.M. Oyvind, Anthocyanins from mauve flowers of Erlangea tomentosa (Bothriocline longipes) based on erlangidin – the first reported natural anthocyanidin with C-ring methoxylation, Photochem. Letters 29 (2019) 225–230.
[20] J. Namukobe, Analysis of Anthocyanins from Fruits of Lea Guineensis and Flowers of acanthus Pubscence, 2006.
[21] J. Namukobe, Analysis of Anthocyanins from Fruits of Lea Guineensis and Flowers of acanthus Pubscence, Unpublished Master's Thesis, Department of Chemistry,Makerere University, 2006.
[22] S. Wahyuningsih, L. Wulandari, M. Wartono, H. Munawaroh, A. Ramelan, The effect of pH and Color stability of anthocyanin on food colorant, in: IOP Conference Series: Materials Science and Engineering, 2017.
[23] S. Sunita, S. Bulkesh, S. Ghoshal, M. Devendra, Dye sensitized solar cells: from genesis to recent drifts, Renew. Sustain. Energy Rev. 2017 (2017) 529–537.
[24] A. Lim, N. Kumara, T.L. Ai, A.H. Mirza, R. Chandrakanthi, M.P. Iskandar, M.C. Lim, G. Senadeera, P. Ekanayake, Potential of natural sensitizers extracted from the skin of canarium odontophyllum fruits for dye sensitized solar cells, Spectrochim. Acta Mol. Biomol. Spectrosc. 138 (2015) 596–602.
[25] V. Shanmugan, S. Manoharan, S. Anandan, R. Murugan, Performance of dye-sensitized solar cells fabricated with extracts from fruits of ivy gourd and flowers of red frangipani as sensitizers, Spectrochim. Acta Mol. Biomol. Spectrosc. 104 (2013) (2013) 35–40.
[26] S. Sarwar, W.K. Ko, J. Han, C.H. Han, Y. Jun, S. Hong, Improved long-term stability of dye-sensitized solar cell by zeolite additive in electrolyte, Electrochim. Acta (2017).
[27] R. Katoth, A. Furube, Electron injection efficiency in dye-sensitized solar cells, J. Photochem. Photobiol., A C 20 (2014) 1–16.
[28] Z. Ning, Y. Fu, H. Tian, Improvement of dye-sensitized solar cells: what we know and what we need to know, Royal Soc. Chem. (2010) 1170–1181.
[29] R.R. Sonia, E.M. Barea, S.F. Fabregat, Analysis of the origin of open circuit voltage in dye solar cells, J. Phys. Chem. Lett. 3 (2012) 1629–1634.
[30] P. Alagarsamy, J. Kandasamy, B. karuppapillai, Interfacial Engineering in Fucntional Materials for Dye Sensitized Solar Cells, 111 River Street, John Wily & Sons Inc., Hobokon,NJ 07030,USA, 2020.
[31] Creative Commons Corporation, Creative commons, Creat. Commons Corp. (November 2013) [Online]. Available: https://creativecommons.org/licenses/by/4.0/. (Accessed 14 March 2021).
[32] N.T.R.N. Kumara, A. Lim, C.M. Lim, P.M. Iskandar, P. Ekanayake, Recent progress and utilization of natural pigments in dye sensitized solar cells:A review, Renew. Sustain. Energy Rev. 17 (2017) (2017) 301–317.
[33] S.F. Fabregat, G.G. Belmonte, I.M. Sero, J. Bisquert, Characterization of nanostructured hybrid and organic solar cells by impedance spectroscopy, Phys. Chem. Chem. Phys. 13 (2011) 9083–9118.
[34] M. Younas, K. Harrabi, Performance enhancement of dye sensitized solar cells via co sensitization of ruthenium(II) based N749 dye and organic sensitizer RK1, Sol. Energy (2020) 260–266.
[35] A. Lasia, Electrochemical Impednace Spectroscopy and its Applications, Springer, New York, 2014.
[36] M. Adachi, M. Sakamoto, J. Jiu, Y. Ogata, I. Seiji, Determination of parameters of electron transport in dye sensitized solar cells using electrochemical impedance spectroscopy, J. Phys. Chem. B 110 (2006) 13872–13880.
[37] A.S. Bondarenko, G.A. Ragoisha, in: Progress in Chemometrics Research Pomerantsev A.L., Nova Science, New York, 2005, pp. 89–102.
[38] W. Aloui, A. Ltaief, A. Bouaziz, Electrical impedance studies of optimized standard P3HT:PC70BM organic bulk heterojunctions solar cells, Superlattice. Microst. (2014) 416–423.
[39] R. Ramaoorthy, K. Karthika, M.A. Dayana, V. Maheswari, N. Pavithra, S. Anandan, V.R. Williams, Reduced Graphene oxide embedded titanium dioxide nanocomposites as novel photoanode material in natural dye sensitized solar cells, J. Mater. Sci. Mater. Electron. (2017).
[40] R.R. Sonia, S.F. Frabregat, Temperature Effect in dye sensitized solar cells, Phys. Chem. Chem. Phys. 15 (2013) 2328.
[41] A. Sacco, Electrochemical impedance spectroscopy: fundamentals and applications in dye sensitized solar cells, Renew. Sustain. Energy Rev. (2017) 814–829.